Research Article

Advances in Mechanical Engineering

Advances in Mechanical Engineering
2018, Vol. 10(3) 1–9
© The Author(s) 2018
DOI: 10.1177/1687814018763178
journals.sagepub.com/home/ade
SAGE

Rotary ultrasonic machining of rocks: An experimental investigation

PKSC Fernando[1], Meng Zhang[1] and Zhijian Pei[2]

Abstract

Rock drilling is widely used to explore and mine energy resources. It has also been used to extract samples to study the earth's geological composition and topography and to explore different planets. Percussive drilling is, as of right now, the most commonly used rock drilling method. Due to the high hardness and abrasiveness of rock, tool wear in rock drilling is severe, thus limiting its penetration rate and resulting in high cost. Therefore, it is crucial to develop more cost-effective rock drilling processes. Rotary ultrasonic machining has been used to drill many materials including metal alloys, ceramics, and composites, and its cost advantages have been demonstrated in many previous studies. This article presents the first experimental investigation of rotary ultrasonic machining of rocks. Three types of rocks (basalt, marble, and travertine) were used. Six input variables (tool rotation speed, feedrate, ultrasonic power, abrasive size, abrasive concentration, and drill bit diameter) were examined and two output variables (cutting force and surface roughness) were measured. Results indicate that rotary ultrasonic machining can drill holes of high quality on rocks of different hardness with a much lower cutting force and at a penetration rate of approximately three times faster than percussive drilling.

Keywords

Basalt, marble, rock drilling, rotary ultrasonic machining, travertine

Date received: 4 September 2017; accepted: 8 February 2018

Handling editor: Shan-Tung Tu

Introduction

Rock drilling is widely used in geoengineering, rock engineering, petroleum engineering, mining, and tunnel engineering.[1] It is also used to collect samples to analyze polar ice sheets and search for life on Mars.[2,3] During the initial development of rock drilling, the penetration rate was primarily dependent on the power of the drilling machines.[4] Today, however, the limiting factor of penetration rate is the severe tool wear from rock drilling,[4,5] which is caused by the high hardness and abrasiveness of the rocks and the possible long-term exposure to multiple rock types during a single drilling process.[6] If the penetration rate were doubled, the estimated yearly cost of US$1200 million for hard rock drilling in the United States could be significantly reduced by US$200–US$600 million.[7] Therefore, it is crucial to develop more cost-effective rock drilling processes.

Percussive drilling is the most commonly used drilling method. It has a higher penetration rate than the conventional rotary or diamond drilling.[1] Tang et al.[8] and Lu et al.[9] studied a new method of rock drilling by combining the traditional mechanical drilling with an

[1]Department of Industrial and Manufacturing Systems Engineering, Kansas State University, Manhattan, KS, USA
[2]Department of Industrial and Systems Engineering, Texas A&M University, College Station, TX, USA

Corresponding author:
Meng Zhang, Department of Industrial and Manufacturing Systems Engineering, Kansas State University, Manhattan, KS 66506, USA.
Email: meng@ksu.edu

assistance of abrasive water jet. This method increased the drilling depth and decreased the axial force, torque, and tool wear.[8,9] Clydesdale et al.[10] developed a core drill bit for the core drilling of rocks, which reduced the fluid invasion and resulted in a higher penetration rate compared to that when using a conventional polycrystalline diamond compact core bit.

Core drilling produces an annular shape cut, which helps in excavating cylindrical cores. Cylindrical cores, as the expected subsurface scientific samples, are used to explore geologic formations, climate histories, biota, and solar activity in terrestrial and extraterrestrial environments.[11] Future extraterrestrial exploration (i.e. on Mars) requires core drilling to collect materials from the subsurface for scientific analysis.[2,3,12] However, extraterrestrial drilling has many constraints such as the extreme environmental conditions and the necessity of complex autonomous systems to acquire cores.[13,14] There is a growing interest in Mars exploration mission to acquire and return subsurface samples as solid cores to the earth for further analyze.[13] Recent studies showed that a combination of conventional drilling techniques with ultrasonic vibration can address the key shortcomings of the drilling in planetary exploration missions.[12,15]

Machining processes that employ ultrasonic vibration as an assistance can be divided into two main categories: ultrasonic machining (USM) and rotary ultrasonic machining (RUM). USM removes material by the abrasive particles in the form of slurry that accelerated and vibrated by the tool. The material removal mechanisms of USM are the impact action of abrasive particles and the hammering action of abrasive particles that removes material by micro-chipping and mechanical abrasion. RUM is a hybrid of USM and abrasive grinding. The main difference between RUM and USM is that RUM uses a metal-bonded diamond abrasive core drill with tool rotation. In addition, Bar-Cohen et al.[15] developed a new ultrasonic drilling and coring device based on USM to drill a wide range of rocks without tool rotation. This device can be performed with low preload (<10 N) and low power (average of 5 W consumption).[15]

A schematic of RUM is shown in Figure 1. The cutting tool is a metal-bonded diamond abrasive core drill. Coolant flows through the core drill to the cutting interface to flush away the removed material and to maintain a low tool temperature. Previous studies have shown that RUM can attain a higher material removal rate than both USM and diamond grinding.[16–18] RUM can also drill deep holes with high accuracy, improved surface finish, and low cutting force and torque.[19] RUM could offer a great advantage in core drilling for future extraterrestrial exploration as opposed to ultrasonic drilling and coring device and USM because of its hybrid material removal mechanism. However, most of the reported studies on RUM have been related to

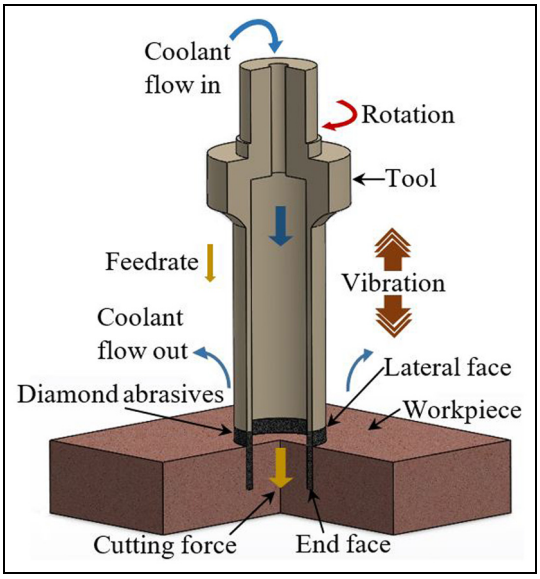

Figure 1. Schematic of rotary ultrasonic machining.

engineering materials (e.g. stainless steel, titanium alloy, composite materials, ceramic materials, and glass). Since natural rocks represent a large group of brittle materials, and RUM has been successfully applied to the machining of many brittle engineering materials, studying the feasibility and the material removal mechanism in RUM of natural rocks will broaden the application of RUM and in the meanwhile shed light on the study of material removal mechanism based on the brittle fracture criteria.

This investigation reports RUM of natural rocks, which are inhomogeneous materials. This research, for the first time, reports feasibility and experimental studies on this new application. In this study, three types of rocks (basalt, marble, and travertine) were used, six input variables (tool rotation speed, feedrate, ultrasonic power, abrasive size, abrasive concentration, and drill bit diameter) were examined, and two output variables (cutting force and surface roughness) were measured. The remainder of this article is presented as follows: section "Experimental conditions and procedures" lists experimental conditions and procedures including the materials, experimental setup, design of experiments, and measurement procedures; section "Experimental results" describes experimental results, including the effects of six input variables on cutting force and surface roughness; finally, section "Conclusion" presents conclusions.

Experimental conditions and procedures

Workpiece materials and properties

There are three main categories of rocks: sedimentary, metamorphic, and igneous. In this study, three types of rocks were chosen to represent the categories. They

Table 1. Properties of rocks.[20]

Property	Unit	Basalt	Marble	Travertine
Density	kg/m^3	2900–3100	2400–2700	2700
Mohs hardness	–	6	3–4	3–4
Abrasion resistance	–	High	Medium	Low
Porosity	–	Low	Low	High

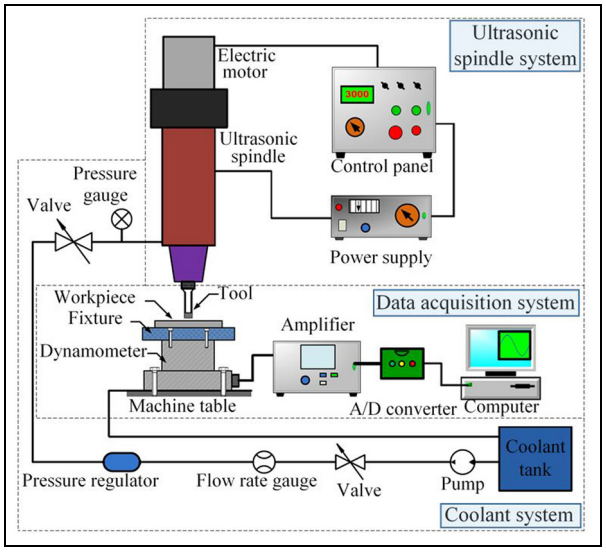

Figure 2. Experimental setup.

were basalt (high strength) from the igneous category, marble (medium strength) from the metamorphic category, and travertine (low strength) from the sedimentary category. Workpiece dimensions were 15 mm × 300 mm × 25 mm. Properties of the three types of rocks are shown in Table 1.

Experimental setup and conditions

The experiments were conducted on a rotary ultrasonic machine (Series 10, Sonic-Mill, Albuquerque, NM, USA). Figure 2 shows a schematic of the experimental setup, which consists of an ultrasonic spindle system, a coolant system, and a data acquisition system. The ultrasonic spindle system was comprised of an ultrasonic spindle, a power supply, an electric motor, and a control panel. The power supply converted the low-frequency (60 Hz) electrical power into a high-frequency (20,000 Hz) AC output that was then converted into mechanical vibrations by the piezoelectric transducer in the ultrasonic spindle. The coolant system was comprised of a pump, coolant tank, pressure regulator, flow rate and pressure gauges, and valves and provided coolant to the spindle and the interface of machining. The data acquisition system was comprised of a dynamometer, a charge amplifier, an analog to digital converter, and software to collect cutting force data.

Experimental conditions

Six input variables, as listed in Table 2, were studied. The effective cutting area (A) of a drill bit is calculated using the formula: $A = (\pi/4) \times (D_o^2 - D_i^2)$, where D_o and D_i are the outer and inner diameters of a drill bit, respectively. Drill bit diameters were selected to keep the difference between the effective cutting areas of two consecutive drill bit diameters about the same.

Experimental conditions are listed in Table 3. Abrasive size indicates the average diameter of the abrasives bonded to cutting tool. Abrasive concentration is based on the weight of diamond per cm^3 (the base value of 100 concentration is 4.4 carat/cm^3). Three replicates were used for each experimental condition, and the output variables were cutting force and surface roughness.

Experimental conditions are listed in Table 3. Three replicas were used for each experimental condition, and the output variables were cutting force and surface roughness.

Measurement procedures

A dynamometer (Kistler 9272, Kistler Instrument Corp., Winterthur, Switzerland) was used to measure the cutting force along the tool axis (feedrate) direction, and the workpiece was mounted on top of the fixture of the dynamometer. Bolts were used to attach the dynamometer to the machine table, as shown in Figure 2. A charge amplifier (Kistler 5070, Kistler Instrument Corp., Winterthur, Switzerland) was used to amplify the signal from the dynamometer, and analog-to-digital converter (PCIM-DAS 1602/16, Measurement Computing Corporation, Norton, MA, USA) was used to convert the signal to a digital signal. The cutting force data were recorded using the DynoWare software (Version 2.4.1.6 type 2825A-02, Kistler Instrument Corp., Winterthur, Switzerland).

Surface roughness of the machined rods was measured using a surface profilometer (Mitutoyo SJ-400, Mitutoyo Corporation, Kanagawa, Japan). The

Table 2. Input variables and their levels.

Input variable	Unit	Level 1	Level 2	Level 3
Tool rotation speed	r/min	1500	2500	3500
Feedrate	mm/s	0.1	0.3	0.5
Ultrasonic power	%	20	40	60
Abrasive size	mm	0.08	0.12	0.16
Abrasive concentration	–	50	100	150
Drill bit outer, inner diameters (D_o, D_i)	mm	(9, 7)	(12, 10)	(15, 13)
Drill bit effective cutting area (A)	mm^2	25.13	34.56	43.98

Table 3. Experiment conditions.

Test order	Tool rotation speed (r/min)	Feedrate (mm/s)	Ultrasonic power (%)	Abrasive size (mm)	Abrasive concentration	Drill bit diameter D_o, D_i (mm)
1	1500	0.3	40	0.12	100	12, 10
2	2500	0.3	40	0.12	100	12, 10
3	3500	0.3	40	0.12	100	12, 10
4	2500	0.1	40	0.12	100	12, 10
5	2500	0.5	40	0.12	100	12, 10
6	2500	0.3	20	0.12	100	12, 10
7	2500	0.3	60	0.12	100	12, 10
8	2500	0.3	40	0.08	100	12, 10
9	2500	0.3	40	0.16	100	12, 10
10	2500	0.3	40	0.12	50	12, 10
11	2500	0.3	40	0.12	150	12, 10
12	2500	0.3	40	0.12	100	9, 7
13	2500	0.3	40	0.12	100	15, 13

Table 4. Experimental results.

Run order	Travertine cutting force (N)	Marble cutting force (N)	Marble, R_a (μm)	Basalt cutting force (N)	Basalt, R_a (μm)
1	56.11	53.45	2.06	93.02	0.78
2	65.04	39.81	2.10	79.52	0.98
3	50.72	36.53	1.92	61.42	0.78
4	51.50	33.25	1.82	55.31	0.92
5	75.53	47.40	1.81	106.66	0.65
6	53.96	47.40	1.80	60.26	0.95
7	65.42	38.58	2.11	75.18	0.99
8	69.54	64.91	1.67	88.60	1.04
9	63.49	59.12	1.18	96.09	1.03
10	58.34	41.93	1.53	93.75	0.91
11	73.27	54.69	1.15	93.68	0.79
12	39.87	32.89	1.19	71.65	0.80
13	97.83	64.99	1.66	130.66	0.89

sampling range was set as 4 mm, and the surface roughness was characterized by the average surface roughness value (R_a). Rock drilling by RUM produced a hole and a rod after each drilling process, and the surface roughness was measured on the cylindrical surface of the extracted rod at the entrance and exit locations along the axial direction of the rod. Four measurements were taken at each quadrant, as shown in Figure 3, and eight R_a values were obtained for each test. The mean and standard deviation of these eight R_a values are reported in this article (section "Experimental results"). Table 4 lists the average values of the measurements.

Experimental results

Effects on cutting force

Cutting force is the predominant output variable in RUM. Cutting force has a significant impact on other

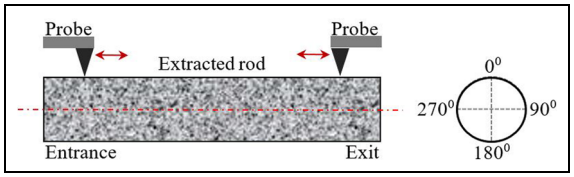

Figure 3. Schematic of surface roughness measurement procedure.

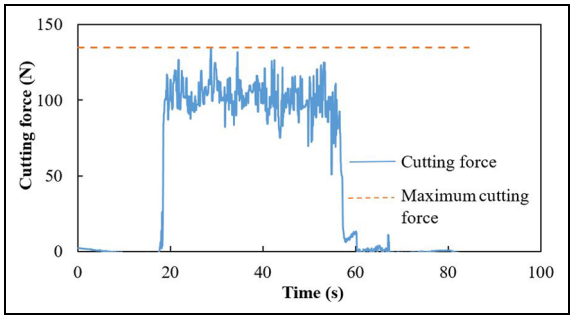

Figure 4. A typical cutting force curve obtained during RUM.

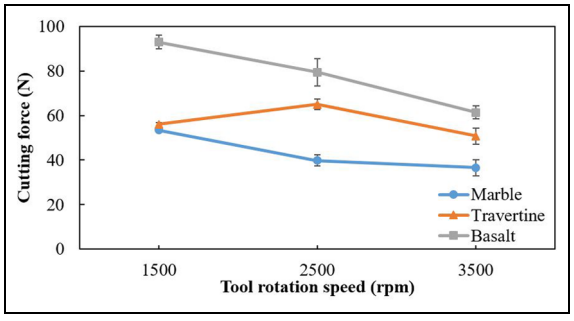

Figure 5. Effects of tool rotation speed on cutting force.

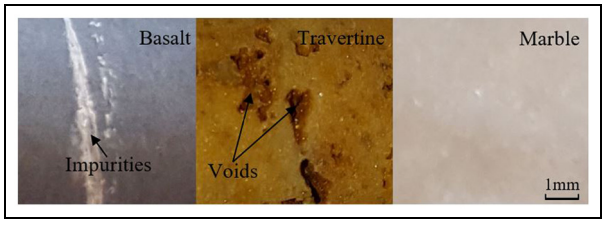

Figure 6. Rock surfaces of machined rods extracted by RUM.

output variables such as tool wear and cutting temperature.[9,21] Figure 4 shows a typical curve of measured cutting force. The maximum cutting force for each test was used in this article. Table 4 presents experimental results on cutting force and surface roughness.

The effects of tool rotation speed, feedrate, ultrasonic power, abrasive size, abrasive concentration, and drill bit diameter on cutting force are shown in Figures 5–11. The mean values of cutting force are presented with the corresponding standard deviations as the error bars.

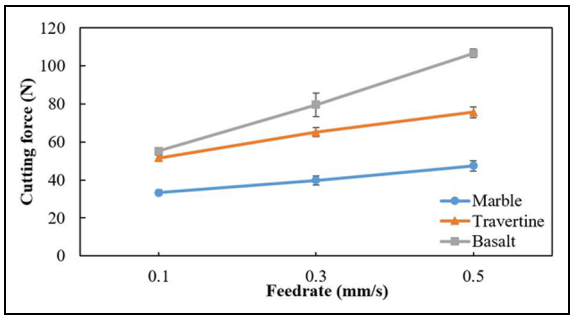

Figure 7. Effects of feedrate on cutting force.

As shown in Figure 5, cutting force decreased for marble and basalt as tool rotation speed increased. The cutting force in RUM mainly depends on the interaction force between diamond abrasives on the tool end surface and the workpiece material.[22] This interaction force increases as penetration depth of diamond abrasives increases.[22] When tool rotation speed increases, this penetration depth tends to decrease when the feedrate is fixed, hence reducing the interaction force.[22] This leads to a reduction in the cutting force.[22] Whereas cutting force increased for travertine as tool rotation speed increased. This outcome for travertine was consistent with previous reports on RUM of other materials including carbon fiber–reinforced plastic composites, sapphire, and dental ceramics.[22–24] For travertine, the increased cutting force associated with the increase in tool rotation speed from 1500 to 2500 r/min was similar to that of RUM of ceramic matrix composites.[18] As shown in Figure 6, travertine was the most porous material; it contained extensive impurities as proven by the dark spots that indicate a different type of rock.

When feedrate increases the penetration depth of diamond abrasives increases, and as a result, interaction force increases. This results in an increase in cutting force. Figure 7 illustrates that cutting force increased as per a close-to-linear trend within the feedrate ranging from 0.1 to 0.5 mm/s. This trend was consistent with previous RUM studies of drilling carbon fiber–reinforced plastics, ceramic matrix composites, and ceramics.[18,19,22]

Ultrasonic vibration amplitude increases as ultrasonic power increases, resulting in an increase in the penetration depth of diamond abrasives into the workpiece material, hence increasing the interaction force. This also results in an increase in cutting force. But as shown in Figure 8, the increasing ultrasonic power caused cutting force to decrease only for marble. For travertine, cutting force increased with an increase in ultrasonic

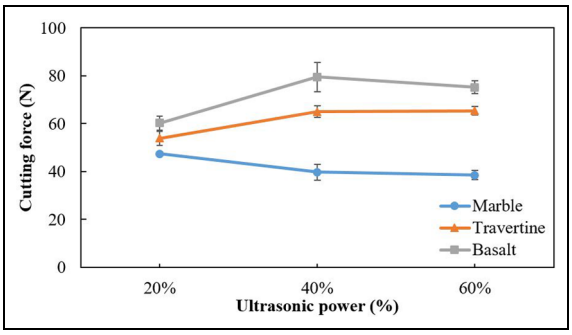

Figure 8. Effects of ultrasonic power on cutting force.

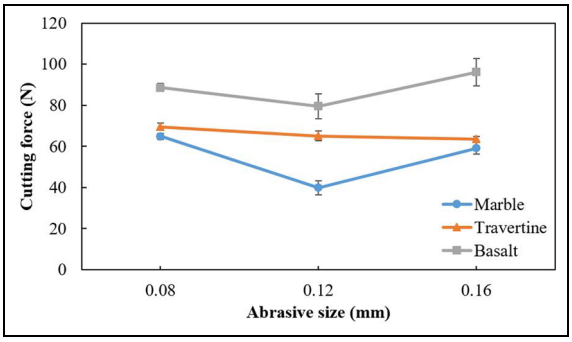

Figure 9. Effects of abrasive size on cutting force.

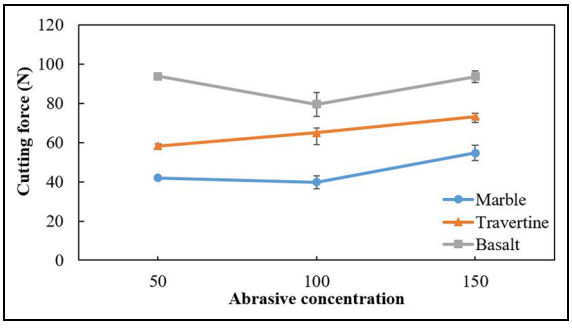

Figure 10. Effects of abrasive concentration on cutting force.

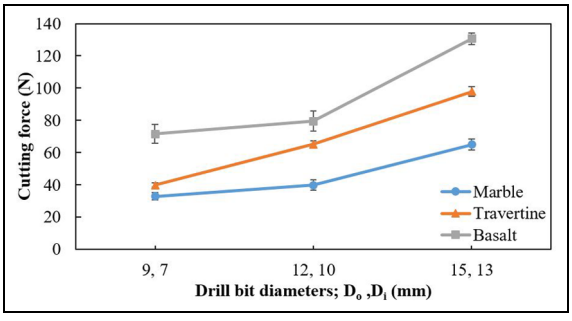

Figure 11. Effects of drill bit diameters on cutting force.

power and basalt showed a peak cutting force at 40% ultrasonic power. Cong et al.[25] reported that when ultrasonic power was set at 20%–40%, the peak cutting force was obtained at 30% ultrasonic power for RUM of stainless steel, which is similar to the behavior of basalt.

When abrasive size increases, penetration depth of diamond abrasives decrease if the ultrasonic power is a constant, hence reducing the interaction force. This results in a reduction in cutting force. Figure 9 shows that the cutting force of travertine decreased as abrasive size increased. Basalt and marble obtained the minimum cutting force at an abrasive size of 0.12 mm. Cong et al.[26] reported that cutting force decreased as abrasive size increased, which was consistent with the reported trend for travertine in this study.

As shown in Figure 10, cutting force had a positive correlation with abrasive concentration only for travertine. Basalt and marble showed the minimum cutting force at an abrasive concentration of 100.

Cutting force increased as drill bit diameter increased for all three rock types as shown in Figure 11. The increment of cutting force from drill bit diameters (9, 7) mm to drill bit diameters (12, 10) mm was much lower than the increment of cutting force from drill bit diameters (12, 10) mm to drill bit diameters (15, 13) mm, despite the difference between the effective cutting areas of the two drill bits being constant.

The highest cutting force was recorded when drilling basalt, which was the hardest rock in the study. RUM can drill holes of 15 mm or smaller in diameter in hard rocks with a cutting force of less than 150 N and a feedrate of 0.5 mm/s. One study on the optimization of rotary-percussion drill for lunar exploration reported that a minimum of 399 N cutting force was obtained when drilling a 33-mm diameter hole in marble.[27] They obtained a penetration rate of 0.17 mm/s at a percussion frequency of 20 Hz.[27] RUM of a 15-mm diameter hole on marble could reach a feedrate of 0.5 mm/s with a cutting force of 64.99 N. Therefore, RUM could offer improved performance over rotary-percussion drilling when drilling rocks such as marble.

Effects on surface roughness

Figures 12–17 show the effects of tool rotation speed, feedrate, ultrasonic power, abrasive size, abrasive concentration, and drill bit diameters on surface roughness. Consistent surface roughness values were impractical to obtain for travertine due to its high porosity (Figure 6). Thus, surface roughness measurements of travertine were not presented in this study as the measured local surface roughness might misrepresent the surface roughness of the machined surface of the travertine workpiece.

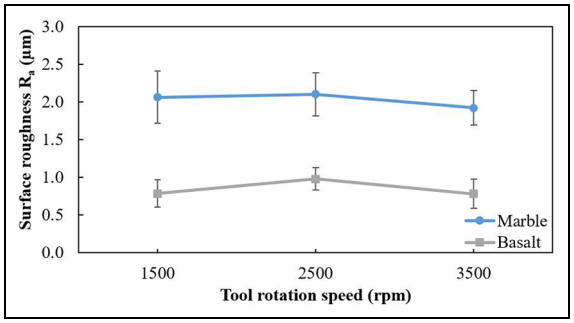

Figure 12. Effects of tool rotation speed on surface roughness.

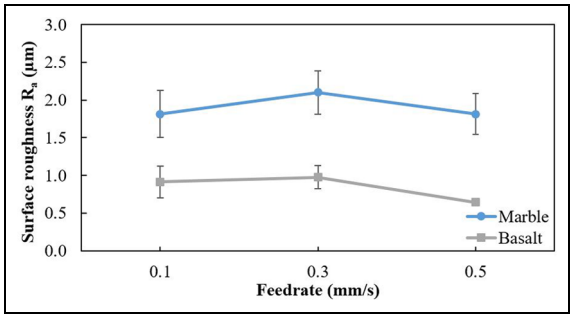

Figure 13. Effects of feedrate on surface roughness.

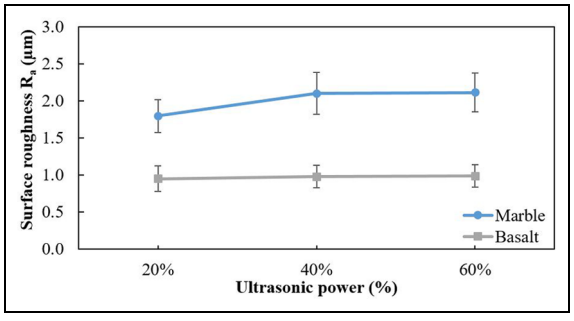

Figure 14. Effects of ultrasonic power on surface roughness.

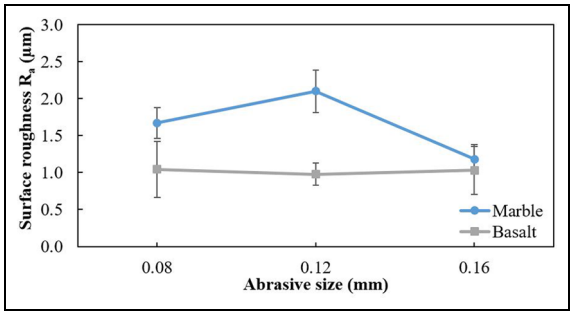

Figure 15. Effects of abrasive size on surface roughness.

As shown in Figure 12, the highest surface roughness was reported at a tool rotation speed of 2500 r/min for basalt and marble. The surface roughness ranges of basalt and marble were 0.18 and 0.20 μm, respectively.

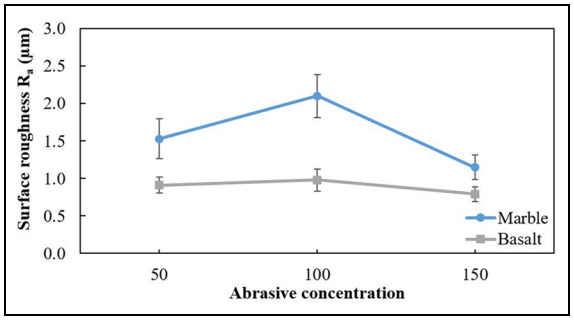

Figure 16. Effects of abrasive concentration on surface roughness.

As shown in Figure 14, ultrasonic power had an insignificant effect on the surface roughness of basalt. The three measurements of surface roughness at each level of ultrasonic power were all within the range of 0.95 and 0.99 μm. Marble showed a direct, positive correlation between surface roughness and ultrasonic power, but the range was only 0.31 μm. Jiao et al.[19] reported that ultrasonic power did not significantly affect surface roughness in RUM of ceramics, as confirmed by the obtained results for basalt in this study.

As shown in Figure 15, the surface roughness of basalt had overlapping error bars, indicating that abrasive size had a statistically insignificant effect on the surface roughness of basalt. However, abrasive size did have a significant effect on the surface roughness of marble, with the highest surface roughness being observed when using the 0.12-mm abrasive size followed by the 0.08- and 0.16-mm abrasive sizes. For basalt and marble, surface roughness values were similar (only differing by 0.15 μm) when using the 0.16-mm abrasive size. According to Jiao et al.,[19] abrasive size had a significant effect on surface roughness for RUM of ceramics, as agreed upon by the obtained results for marble in this study.

As shown in Figure 16, abrasive concentration had more influence on the surface roughness of marble than basalt. A smoother surface finish was obtained when using the highest abrasive concentration of 150 for both rocks. Higher abrasive concentration means that a larger number of abrasive particles were involved in cutting, which produces smaller chips and finer scratches on the surface, resulting in a better surface finish.

As shown in Figure 17, drill bit diameters significantly affected surface roughness, especially for marble. The smallest drill bit resulted in the best surface finish for both rock types. However, drill bit diameters had a minor effect on the surface roughness for basalt. For both rock types, the highest surface roughness was reported for the drill bit with the outer and inner diameters of 12 and 10 mm, respectively.

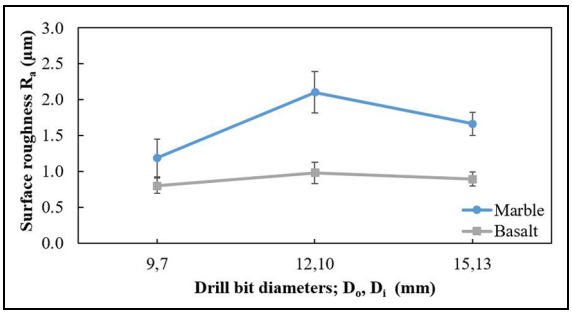

Figure 17. Effects of drill bit diameters on surface roughness.

Conclusion

This article presents an experimental study on RUM of three types of rocks: basalt, travertine, and marble. The following conclusions are drawn:

1. This investigation demonstrated that RUM is capable of drilling hard rocks with a feedrate comparable to that of existing drilling procedures.
2. The effects of feedrate and drill bit diameter on cutting force were significant. A higher feedrate and larger drill bit diameter led to a higher cutting force.
3. For basalt and marble, an abrasive concentration of 100 gave the lowest cutting force and cutting force decreased as tool rotation speed increased.
4. Tool rotation speed, feedrate, and ultrasonic power had an insignificant effect on surface roughness.

Declaration of conflicting interests

The author(s) declared no potential conflicts of interest with respect to the research, authorship, and/or publication of this article.

Funding

The author(s) disclosed receipt of the following financial support for the research, authorship, and/or publication of this article: Publication of this article was funded, in part, by the Kansas State University Open Access Publishing Fund.

ORCID iD

Meng Zhang https://orcid.org/0000-0002-9220-7193

References

1. Bruno MS. Fundamental research on percussion drilling: improved rock mechanics analysis, advanced simulation technology, and full-scale laboratory investigations. Technical report, Department of Energy, Washington, DC, 31 December 2005.
2. Garry JRC and Wright IP. Coring experiments with cryogenic water and carbon dioxide ices-toward planetary surface operations. *Planet Space Sci* 2004; 52: 823–831.
3. Stocker CR, Cannon HN, Dunagen SE, et al. The 2005 MARTE robotic drilling experiment in Rio Tinto, Spain: objectives, approach, and results of a simulated mission to search for life in the Martian subsurface. *Astrobiology* 2008; 8: 921–945.
4. Beste U. *On the nature of cemented carbide wear in rock drilling*. PhD Thesis, Uppsala University, Uppsala, 2004.
5. Beste U, Hartzell T, Engqvist H, et al. Surface damage on cemented carbide rock-drill buttons. *Wear* 2001; 249: 324–329.
6. Hawk JA and Wilson RD. *Modern tribology handbook*. New York: Springer, 2001, pp.1331–1370.
7. Tibbitts GA, Tek T, Long RC, et al. World's first benchmarking of drilling mud hammer performance at depth conditions. In: *Proceedings of the IADC/SPE drilling conference*, Dallas, TX, 25–28 February 2002, paper no. SPE-74540-MS. Richardson, TX: Society of Petroleum Engineers.
8. Tang J, Lu Y, Ge Z, et al. A new method of combined rock drilling. *Int J Mining Sci Technol* 2014; 24: 1–6.
9. Lu Y, Tang J, Ge Z, et al. Hard rock drilling technique with abrasive water jet assistance. *Int J Rock Mech Min* 2013; 60: 47–56.
10. Clydesdale G, Leseultre A and Lamine E. Low invasion corehead reduces mud invasion while improving performances. *Oil Gas J* 1994; 92: 51–57.
11. Zacny K, Bar-Cohen Y, Brennan M, et al. Drilling systems for extraterrestrial subsurface exploration. *Astrobiology* 2008; 8: 665–706.
12. Beaty D, Miller S, Zimmerman W, et al. Planning for a Mars in situ sample preparation and distribution (SPAD) system. *Planet Space Sci* 2004; 52: 55–66.
13. Zacny K and Cooper G. Considerations, constraints and strategies for drilling on Mars. *Planet Space Sci* 2006; 54: 345–356.
14. Tang J, Quan Q, Jiang S, et al. A soil flowing characteristics monitoring method in planetary drilling and coring verification experiments. *Adv Space Res* 2017; 59: 1341–1352.
15. Bar-Cohen Y, Sherrit S, Dolgin B, et al. Ultrasonic/sonic drilling/coring (USDC) for in-situ planetary applications. In: *Proceedings of the SPIE smart structures conference*, Newport Beach, CA, 1–5 March 2000, paper no. 101. Bellingham, WA: SPIE.
16. Prabhakar D. Machining advanced ceramic materials using rotary ultrasonic machining process. MSc Thesis, University of Illinois at Urbana-Champaign, IL, 1992.
17. Hu P, Zhang J, Pei Z, et al. Modeling of material removal rate in rotary ultrasonic machining: designed experiments. *J Mater Process Tech* 2002; 129: 339–344.
18. Li Z, Jiao Y, Deines T, et al. Rotary ultrasonic machining of ceramic matrix composites: feasibility study and designed experiments. *Int J Mach Tool Manu* 2005; 45: 1402–1411.
19. Jiao Y, Hu P, Pei Z, et al. Rotary ultrasonic machining of ceramics: design of experiments. *Int J Manuf Tech Manag* 2005; 7: 192–206.

20. Stone Source. Technical performance specs. Report, Stone Source, New York, 10 October 2012.
21. Fenn O. The use of water jets to assist free-rolling cutters in the excavation of hard rock. *J S Afr I Min Metall* 1987; 87: 137–147.
22. Cong W, Feng Q, Pei Z, et al. Rotary ultrasonic machining of carbon fiber-reinforced plastic composites: using cutting fluid vs. cold air as coolant. *J Compos Mater* 2011; 46: 1745–1753.
23. Zhang C, Feng P, Pei Z, et al. Rotary ultrasonic machining of sapphire: feasibility study and designed experiments. *Key Eng Mater* 2013; 589–590: 523–528.
24. Churi N, Pei Z, Shorter D, et al. Rotary ultrasonic machining of dental ceramics. *Int J Mach Mach Mater* 2009; 6: 270–284.
25. Cong W, Pei Z, Deines T, et al. Rotary ultrasonic machining of stainless steels: empirical study of machining variables. *Int J Manuf Res* 2010; 5: 370–386.
26. Cong W, Pei Z, Sun X, et al. Rotary ultrasonic machining of CFRP: a mechanistic predictive model for cutting force. *Ultrasonics* 2014; 54: 663–675.
27. Jie D, Li P, Quan Q, et al. Optimization of percussive mechanism in rotary-percussion drill for lunar exploration. In: *Proceedings of the* IEEE *international conference on robotics and biomimetics*, Shenzhen, China, 12–14 December 2013, pp.2130–2135. New York: IEEE.